

PAPER • OPEN ACCESS

Voltage-controlled ON switching and manipulation of magnetization via the redox transformation of β -FeOOH nanoplatelets

To cite this article: Martin Nichterwitz *et al* 2020 *J. Phys. D: Appl. Phys.* **53** 084001

View the [article online](#) for updates and enhancements.

Recent citations

- [Special issue on voltage control of nanomagnetism](#)
Jiamian Hu and Massimo Ghidini
- [Voltage-Induced ON Switching of Magnetism in Ordered Arrays of Non-Ferromagnetic Nanoporous Iron Oxide Microdisks](#)
Matteo Cialone *et al*



IOP | ebooks™

Bringing together innovative digital publishing with leading authors from the global scientific community.

Start exploring the collection—download the first chapter of every title for free.

Voltage-controlled ON switching and manipulation of magnetization via the redox transformation of β -FeOOH nanoplatelets

Martin Nichterwitz^{1,2}, Sabine Neitsch¹, Stefan Röher¹, Daniel Wolf¹ , Kornelius Nielsch^{1,3}  and Karin Leistner^{1,3} 

¹ IFW Dresden, Helmholtzstr. 20, 01069, Dresden, Germany

² Faculty of Chemistry and Food Chemistry, TU Dresden, Physical Chemistry, D-01062, Dresden, Germany

³ Faculty of Mechanical Engineering, TU Dresden, Institute of Materials Science, D-01062, Dresden, Germany

E-mail: K.Leistner@ifw-dresden.de

Received 2 September 2019, revised 13 November 2019

Accepted for publication 26 November 2019

Published 13 December 2019



Abstract

Redox-based metal/metal oxide transformations achieved via electrolytic gating recently emerged as a novel, magneto-ionic route for voltage control of magnetism. So far, mainly metal or oxide thin films and nanoporous metal alloy structures are used as starting materials. The present study demonstrates a magneto-ionic transformation starting from a stable electrodeposited FeOOH nanoplatelet structure. The application of a low voltage in a Li-based electrolyte results in the reduction of the virtually non-magnetic FeOOH into ferromagnetic Fe, yielding an ON switching of magnetization. The magnetization can be tuned in a large range by the time of voltage application and remains stable after voltage-switch off. A reversible magneto-ionic change of magnetization of up to 15% is achieved in the resulting iron films with a thickness of about 30 nm. This large magneto-ionic effect is attributed to the enhanced roughness of the iron films obtained from the nanoplatelet structure. The robust, voltage-controlled, and non-volatile ON switching of magnetism starting from a stable oxide structure is promising for the development of energy-efficient magnetic switches, magnetic actuation and may offer new avenues in magnetoelectronic devices.


Keywords: magnetoelectric actuation, magneto-ionic effects, voltage control of magnetism, iron oxyhydroxide, iron films

(Some figures may appear in colour only in the online journal)

1. Introduction

Voltage control of magnetism, compared with other control parameters, such as pressure, temperature, spin polarized current or a magnetic field, promises to boost energy efficiency of magnet-based devices in many areas of nanotechnology. Conventional magnetoelectric effects in multiferroic materials

or magnetic semiconductors are often restricted by a low Curie/Neel temperature (T_C/T_N), low magnetization (M), or the need for high-quality epitaxial interfaces [1]. Significant room temperature magnetoelectric effects can be achieved by exploiting voltage-triggered redox reactions in magnetic nanostructures, the so-called magneto-ionic effect [2–4]. In this case, the voltage is applied to the magnetic surface via a solid dielectric layer or a liquid electrolyte and magnetic changes occur due to charge transfer and associated changes of the chemical composition. This has enabled considerable manipulation of, e.g. magnetization [5–7], magnetic

 Original content from this work may be used under the terms of the [Creative Commons Attribution 3.0 licence](https://creativecommons.org/licenses/by/3.0/). Any further distribution of this work must maintain attribution to the author(s) and the title of the work, journal citation and DOI.

anisotropy [2, 8, 9], coercivity [10, 11], domain wall pinning [3] and exchange bias [12]. In contrast to capacitive electronic charging and most other magnetoelectric approaches that are volatile and require the constant application of voltage, magneto-ionic effects can persist after the voltage has been switched off [12–14]. Due to this nonvolatility, the magnetic state in magneto-ionic materials can ideally be set at will by the external voltage, requiring a small current only for the charge transfer as the setting. This provides a huge potential for improving the energy efficiency of magnetic technologies in computing, spintronics, actuation, and lab on chip devices [4, 15, 16].

To date, such redox-based voltage control of magnetism is mainly studied for ultrathin films with thickness of or below few nanometers [9, 10, 13, 14, 17, 18]. Since the magneto-ionic mechanism is based on interface reactions, an increase of the surface/volume ratio and the use of porous structures are promising routes to the magneto-ionic control of larger structures [5, 6]. Liquid electrolytes are beneficial here, since they can easily infiltrate the structures and they exhibit high ionic mobility. In addition, the formation of the electrochemical double layer in liquid electrolytes makes magneto-ionic effects possible at much lower voltage than in solid electrolytes [16, 19].

The extension of electrochemically controlled magnetism towards bulk has already been achieved via liquid electrolyte gating and Li intercalation for metal organic frameworks [20] and various porous or nanosized metal oxides [21–23]. These materials, however, cannot compete with ferromagnetic metals in terms of magnetization values. Therefore, the combination of porous magneto-ionic materials involving a transformation to a ferromagnetic metal seems attractive. For example, a transformation from non-magnetic Fe_2O_3 nanoparticles to ferromagnetic Fe has been demonstrated using a Li-based non-aqueous liquid electrolyte [24]. In several porous metal alloy systems, voltage-induced magnetization changes are achieved via oxidation/reduction reactions [6, 25]. In these cases, the porous metal oxide/metal alloy structure, which is used as a starting material [6, 25] already contains a ferromagnetic component. This impedes an ON switching of metal ferromagnetism from a complete OFF state, as, e.g. desired for magnetic switches and actuation.

In the present study, long-term stable β -FeOOH (aka-genéite) nanoplatelets in combination with simple alkaline aqueous solution are utilized as virtually non-magnetic and high surface area starting material for magneto-ionic manipulation. So far, β -FeOOH is mainly studied with regard to catalysis and as battery anode material [26, 27]. A high surface/volume ratio is beneficial to achieve a highly electrochemically active FeOOH material, despite the low intrinsic conductivity [28]. We use electrodeposition as an efficient method to achieve nanosized β -FeOOH at room temperature and ambient pressure [26, 28]. The nanoplatelets are then polarized in different alkaline solutions, aiming at a voltage-induced change in magnetism. The associated voltage-induced structural and morphological changes are probed in detail and correlated to the measured magnetic changes. This approach, starting from paramagnetic FeOOH, enables complete and

non-volatile ON switching of ferromagnetic layers and large reversible magneto-ionic effects.

2. Methods

Electrodeposition of β -FeOOH is carried out according to the routine described by Zou *et al* [26] from unstirred aqueous solution of 0.1 M $\text{FeCl}_2 \cdot 4 \text{H}_2\text{O}$ and 0.05 M NaNO_3 . A Si wafer with a thermal oxide of 1 μm and sputtered Au (10 nm)/Cr (4 nm) buffer layers is used as substrate and working electrode. The electrochemical cell is a two electrode cylindrical teflon cell with Pt counter electrode. Galvanostatic deposition is performed at 0.2 mA cm^{-2} on a circular area of 38.5 mm^2 . Deposition times t_{dep} are between 180 s and 600 s.

For the redox-based magneto-ionic transformation starting from the FeOOH deposit, three liquid alkaline electrolytes, 1 M NaOH, 1 M KOH, and 1 M LiOH in aqueous solution, are tested. Cyclic voltammetry (CV) and the potentiostatic electroreduction process are carried out in 3-electrode arrangement with a saturated calomel electrode (SCE) as reference electrode and a Pt wire as the counter electrode. The voltage quoted thus represents the potential E of the working electrode versus SCE.

High-resolution transmission electron microscopy (TEM) is conducted on a double-aberration-corrected FEI Titan³ 80-300 microscope operated at 300 kV to investigate the nanostructure and morphology of the FeOOH nanoplatelets. The phase transformation of the deposits is observed using θ - 2θ x-ray diffraction (XRD, Bruker D8 Advance, Co- $K\alpha$ radiation). The surface and cross section of the as deposited and transformed nanostructures are characterized via scanning electron microscopy (SEM, LEO 15030 Gemini from Zeiss). Atomic force microscopy (AFM, Dimension ICON) in tapping mode is carried out to characterize the surface morphology and roughness.

The magnetic properties are characterized prior and quickly after the voltage-induced redox-transformation via anomalous Hall effect (AHE) measurement in a physical property measurement system (PPMS 6100, Quantum design). A magnetic field $\mu_0 H$ of up to ± 3 T is applied perpendicular to the film plane with a field rate of 20 mT s^{-1} . Simultaneously, a current of 10 mA is applied in the in-plane direction, and the Hall resistance is measured in the orthogonal in-plane direction. The current is expected to flow through the metallic but non-magnetic Au layer, and, after electroreduction, through the metallic ferromagnetic Fe. In ferromagnets, the Hall resistance R_{H} exhibits two contributions: $R_{\text{H}} = R_0 H_{\perp} + R_{\text{S}} M_{\perp}(H)$ [29]. $R_0 H_{\perp}$ (R_0 —normal Hall coefficient) is the normal Hall resistance and $R_{\text{S}} M_{\perp}(H)$ (R_{S} —anomalous Hall coefficient, M_{\perp} —perpendicular component of magnetization) is the anomalous Hall resistance R_{AHE} . In the present case, the $R_{\text{H}}(H)$ curves are corrected for the normal Hall effect. The remaining R_{AHE} curves thus scale with M_{\perp} . Changes in R_{S} are assumed negligible, since the measurements are performed at constant temperature. Therefore, even though absolute values of magnetization cannot be derived, the changes of R_{AHE} are used as a measure for the relative changes in magnetization.

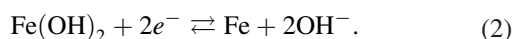
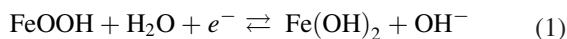
For the reversible magneto-ionic manipulation of the transformed iron layers, *in situ* AHE measurements are performed in a custom-built two-electrode electrochemical cell with a Pt wire as counter electrode. Further *in situ* cell details are described in a previous work [30]. The whole deposit area is exposed to the electrolytic gating, since the *in situ* cell has the same opening dimension for the working electrode as the electrodeposition cell. In some cases, a drift of the AHE curves occurred, which is possibly due to ongoing temperature stabilization and/or reduction/oxidation processes. This drift is less pronounced after magnetic field reversal. Therefore, both for *ex situ* and *in situ* measurements, the branches of the AHE curves from -3 T to $+3$ T are evaluated. The voltages quoted for the *in situ* measurements represent the applied cell voltage.

3. Results and discussion

3.1. Electric ON switching of magnetism via FeOOH nanoplatelet transformation

The electrodeposited FeOOH nanostructure, as shown in figures 1(a), (b) and (d), consists of polycrystalline nanoplatelets with a thickness in the range of few to tens of nanometers and lateral platelet extensions of several hundreds of nanometers. The electron diffraction patterns (figure 1(c)) and the calculated diffractograms from high resolution TEM (figure 1(d)) are consistent with the tetragonal crystal structure of β -FeOOH. The random distribution of the platelets gives rise to the porous and high surface area morphology which is typical for electrodeposited β -FeOOH [26]. The thickness of the porous FeOOH deposit can be tuned by t_{dep} .

The change of the magnetic state by voltage is anticipated by transforming the paramagnetic β -FeOOH [31] to ferromagnetic Fe during electrolytic gating. To achieve the required voltage-triggered reduction reaction, three alkaline aqueous electrolytes, 1 M NaOH, 1 M KOH and 1 M LiOH, are tested. In these electrolytes, the FeOOH to Fe transformation is expected to proceed via the following reactions [32]:



To identify the reactions and chose suitable potentials for the voltage-induced reduction/oxidation, CV is performed for the β -FeOOH samples in the three electrolytes (figure 2). The CV curves start at the open circuit potential (-0.16 V for the NaOH and KOH electrolytes, -0.15 V for the LiOH electrolyte) in cathodic (negative) direction. In all three electrolytes, a cathodic current density (j) peak at -1.00 V appears, which shows the reduction of Fe^{3+} ions present in β -FeOOH to Fe^{2+} ions in $\text{Fe}(\text{OH})_2$ (reaction (1)). For more negative potentials, a strong increase in cathodic j is measured, which is due to the hydrogen ion reduction reaction. In the case of LiOH, an additional shoulder peak at -1.35 V (see inset in figure 2) is observed, which indicates that the desired reduction from Fe^{2+} ions to Fe^0 (reaction (2)) readily occurs. This observation is in line with reports on an easy reducibility of iron oxides in Li-based electrolytes [33]. In the NaOH and KOH

electrolytes, a feature for the Fe^{2+} to Fe^0 reduction reaction is not resolved in the CV; but it may be hidden due to a superposition with the strong hydrogen evolution at more negative potentials. Indeed, macroscopically, the reduction of rusty-red FeOOH to metallic Fe could be observed in all three electrolytes when polarizing at -1.27 V for 180 min. In the CV, after potential reversal, two smaller (positive) j -peaks appear in the anodic scan, which can be ascribed to the re-oxidation of Fe to $(\text{FeOH})_2$ (reverse reaction (1)) and FeOOH (reverse reaction (2)) [32, 34, 35].

The facile electrochemical reduction of nanoplatelet β -FeOOH to Fe at room temperature presents an interesting result on its own. So far, studies on the reduction of iron oxide phases to Fe focus on oxides which naturally occur in iron ores. For example, the electroreduction of Fe_2O_3 to Fe in alkaline electrolytes is described for 100 °C [36]. The room temperature electroreduction of Fe_3O_4 films to iron films in KOH solution has only recently been proposed for the design of layered metal/oxide heterostructures [37]. The present results reveal that the reduction of nanoplatelet β -FeOOH is another viable room temperature route to the fabrication of magnetic iron layers.

For the further experiments targeting the magneto-ionic transformation we chose $E = -1.27$ V applied via the LiOH electrolyte. At this E , the reduction reaction to Fe in LiOH just starts, and the hydrogen evolution reaction is still negligible.

The voltage-induced phase transformation is proven by XRD (figure 3) for an FeOOH sample obtained with $t_{\text{dep}} = 600$ s. For the as deposited state, only the substrate peaks are observed. The FeOOH peaks are not resolved, which is connected to the nanocrystalline and porous nature of the FeOOH deposit. After application of -1.27 V for 180 min, a strong peak at exactly the position of the bcc Fe(1 1 0) reflex is observed. Other bcc Fe peaks are not resolved. As the measurement is carried out in Bragg-Brentano geometry, this shows a preferred orientation of the Fe {1 1 0} planes parallel to the surface. Such a (1 1 0) fiber texture is typical for electrolytic iron films and connected to the low surface energy of the close packed (1 1 0) plane in bcc Fe [38]. The electrolytic transformation can also be followed macroscopically, which is depicted in the inset photographs in figure 3. The color of the deposit changes from the rusty-red FeOOH to metallic-grey iron after voltage application.

The FeOOH to Fe phase transformation goes along with a strong morphological transformation, which becomes evident in the cross section SEM images in figure 4. The starting point is the nanoplatelet structure of as deposited FeOOH (figure 4(a)). Upon voltage application, for increasing reduction times (t_{red}), the platelet structure gradually transforms into a film with granular morphology. After 10 min (figure 4(b)), remains of the platelets are still evident and iron is present in the form of nanosized islands. For longer times (60 min and 180 min, figures 4(c) and (d), respectively), more compact and thicker iron films evolve. An iron film thickness of ca. 28 nm is found after 180 min (figure 4(d)).

This morphology change suggests that the reduction reaction proceeds via a dissolution/redeposition process and

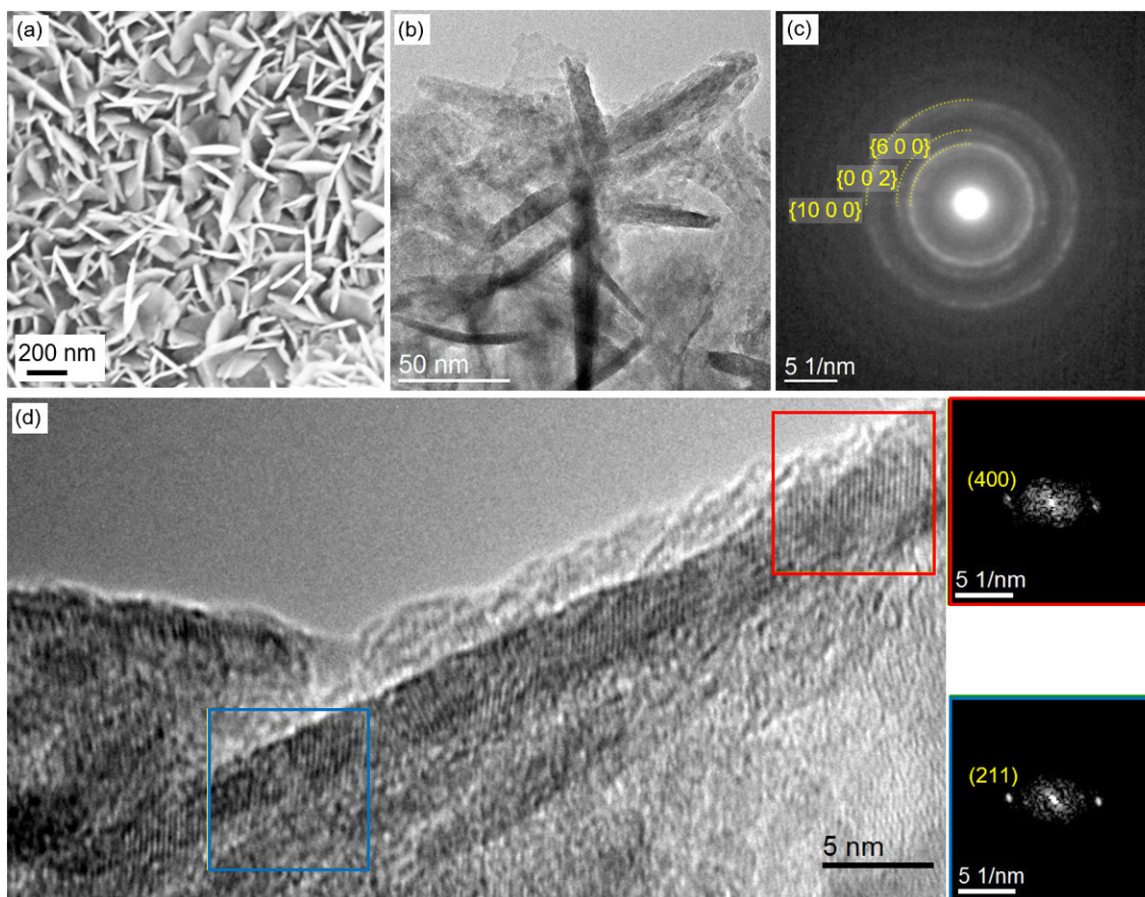


Figure 1. Morphology and structure of electrodeposited nanoporous FeOOH. (a) SEM surface image and (b) bright-field TEM image of the nanoplatelets. (c) Electron diffraction pattern obtained from the nanoplatelet bundle in (b), which reveals Debye-Scherrer-rings consistent with the tetragonal crystal structure of the β -FeOOH nanoplatelets (space group I 4/m 87, ICSD 31136). (d) High resolution TEM image of a platelet exhibiting nanograins that partially show lattice fringes depending on their orientation. The diffractograms on the right are calculated from the subimages marked in (d) and further support the tetragonal β -FeOOH crystal structure.

involves the whole FeOOH structure. Such a mechanism is already under debate for the reduction of Fe_3O_4 to Fe [37]. Indeed, for several iron (oxyhydr-)oxides the dissolution and associated release of Fe^{2+} ions is known upon the application of a reduction potential [39]. We could confirm that the dissolution step does not proceed without voltage application. The FeOOH nanoplatelet structure is stable in the electrolyte in the absence of an external voltage and it thus acts as iron ion reservoir, which can be activated to form a metallic iron layer upon voltage application. Since the starting material is porous, the electrolyte penetrates the whole structure and a large amount of material can be transformed. This may be an advantage over thin film oxides as starting material, since for these the transformed volume is restricted by the reaction layer thickness of few nanometers or below. The AFM image (figure 4(e)) reveals a roughness $Rq = 7.5$ nm for the resulting iron layer. This Rq value presents a lower limit, as the AFM tip is not infinitely sharp and cannot probe all recesses. The roughness is high in comparison to most metal films used for magneto-ionics so far, which are prepared by physical methods [9, 13]. Thus, despite the collapse of the nanoplatelets, a high surface area morphology is still present.

The voltage-induced change in magnetic properties associated with the FeOOH to Fe redox transformation is presented

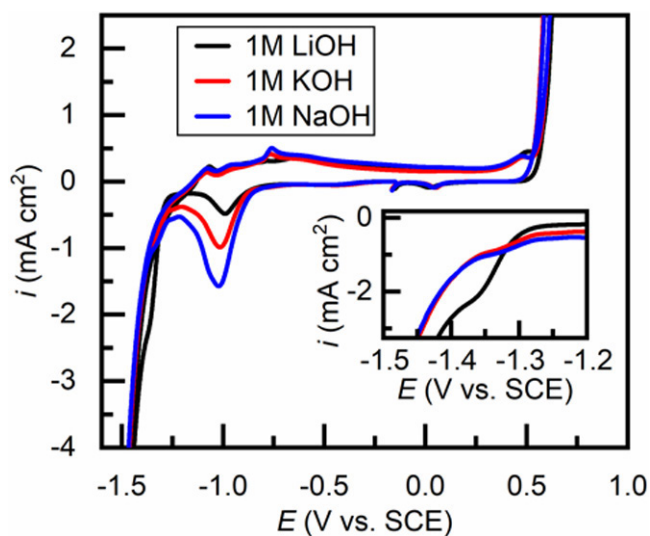


Figure 2. CV of FeOOH samples ($t_{\text{dep}} = 600$ s) in LiOH, KOH, and NaOH aqueous electrolytes. The inset is a magnification showing the shoulder peak assigned to the Fe^{2+} to Fe^0 reduction.

in figure 5. In as deposited FeOOH state, no AHE effect is observed, which is in line with the paramagnetic nature of FeOOH [31]. Upon voltage application, clear AHE signals are

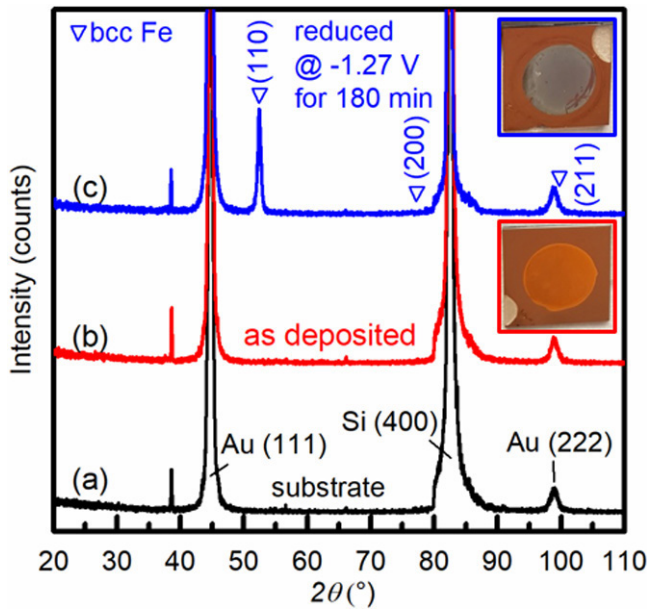


Figure 3. XRD pattern of (a) the Si substrate, (b) the as deposited FeOOH ($t_{\text{dep}} = 600$ s), and (c) the same sample after electrolytic gating at -1.27 V for 180 min. The insets on the right show photographs of the macroscopic surface for (b) and (c) with rusty-red FeOOH and metallic iron, respectively.

observed in figure 5(a). The AHE curves correlate to the out-of-plane magnetization curves of the formed iron layer [5]. As expected for an iron layer, for which the film plane is the magnetic easy plane, the AHE curve shapes signify a continuous rotation of M upon the application of the perpendicular magnetic field. The saturated anomalous Hall resistance ($R_{\text{AHE,S}}$) increases with prolonged t_{red} (figure 5(b)). This increase in $R_{\text{AHE,S}}$ is a measure for the increase in saturation magnetization which accompanies the FeOOH to Fe transformation.

The presented AHE curves in figure 5(a) are measured after voltage switch off and electrolyte removal. This signifies that different magnetic layers, from few to almost 30 nm thick iron films, can be set by voltage in a non-volatile manner. The porosity of the initial FeOOH nanostructure seems crucial for this large magneto-ionic ON switching effect. The reason is that the electrolyte can penetrate into the nanoporous FeOOH and thereby enable a large reactive interface area, where the FeOOH to Fe reduction reaction can proceed. In consequence, the whole FeOOH structure can be transformed into an iron layer with thicknesses of several tens of nanometers. In principle, even larger Fe layer thickness should become possible, when the thickness of the initial FeOOH deposit is increased further. Thus, the FeOOH–Fe transformation enables the voltage-triggered ON switching of a magnetic layer beyond the ultrathin limit.

3.2. Reversible voltage-induced magnetization changes in electrolytic iron films

The full ON switching of magnetism from the FeOOH platelets is a one-time process due to the collapse of the FeOOH structure. The iron films produced by this reduction process, due to their large roughness, are interesting to study reversible

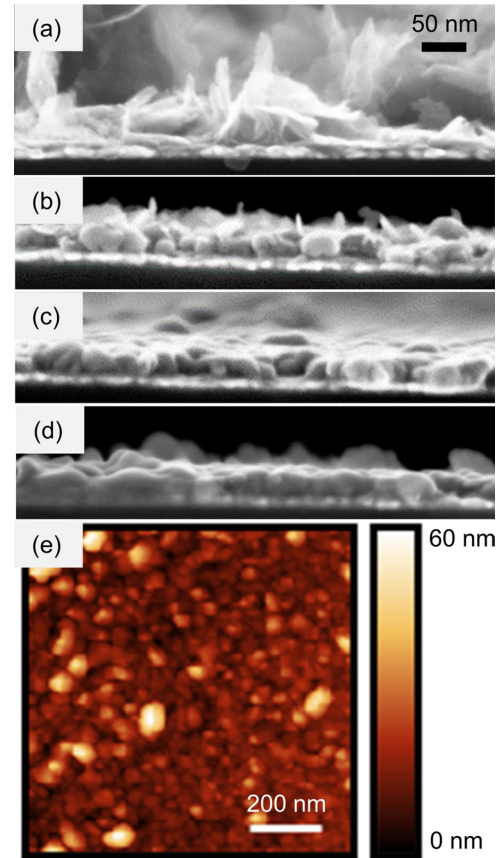


Figure 4. Cross section SEM images (a) of FeOOH in as deposited state ($t_{\text{dep}} = 600$ s) and (b)–(d) after electrolytic reduction of this sample at -1.27 V for (b) 10 min, (c) 60 min and (d) 180 min. (e) AFM image of the thin film depicted in (d).

magneto-ionic magnetization changes. Figure 6 depicts the AHE curves measured for iron films with a thickness of 28 nm (see figure 4(d)) when subjected to voltage-induced reduction and oxidation in 1 M LiOH electrolyte. The cell voltages are chosen according to a previous study on magneto-ionic iron films in LiOH solution [12]. A clear difference in $R_{\text{AHE,S}}$ as a measure for M_S is observed. In the reduced state (at -1.84 V), $R_{\text{AHE,S}}$ is increased in comparison to the state in the oxidation regime (at -0.12 V). This increased M_S at -1.84 V is related to the reduction of the iron oxide surface layer to ferromagnetic iron and in line with previous studies [5, 9]. During re-oxidation at -0.12 V, this surface layer is transformed into iron oxide, associated with a lower M_S . This behaviour is repeatable, as depicted in figure 6(b). The voltage-induced M_S changes lie around 15%. In previous studies, similar and larger magnetization changes up to ON/OFF switching of magnetism are achieved in Co films below 2 nm and in nano-sized iron islands, but the magnetic changes quickly decay when increasing the thickness [5, 14]. In the present study, the significant magnetic change is achieved for a much larger iron film thickness of about 28 nm. This large magneto-ionic effect can be explained by the large surface area in the very rough films (see figure 4(e) and corresponding discussion). The present measurements show that despite the high surface area the films are stable in the alkaline electrolyte for at least 13 measurement cycles, equivalent to a time of 3 h. The drift

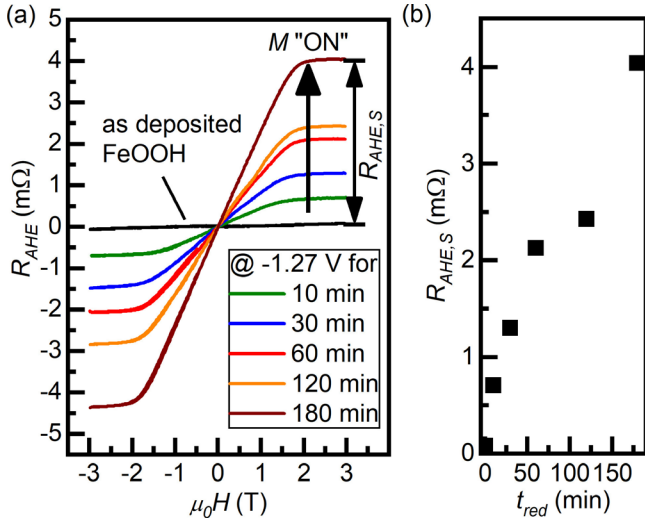


Figure 5. Electric ON switching of magnetism via electrolytic gating of FeOOH deposits ($t_{dep} = 600$ s). (a) Magnetization curves as measured by AHE and (b) $R_{AHE,S}$ at $\mu_0 H = 3$ T extracted from the curves in (a) as measure for M_S after reduction at -1.27 V for different reduction times t_{red} . The measurements are performed within 10 min after voltage switch off and electrolyte removal.

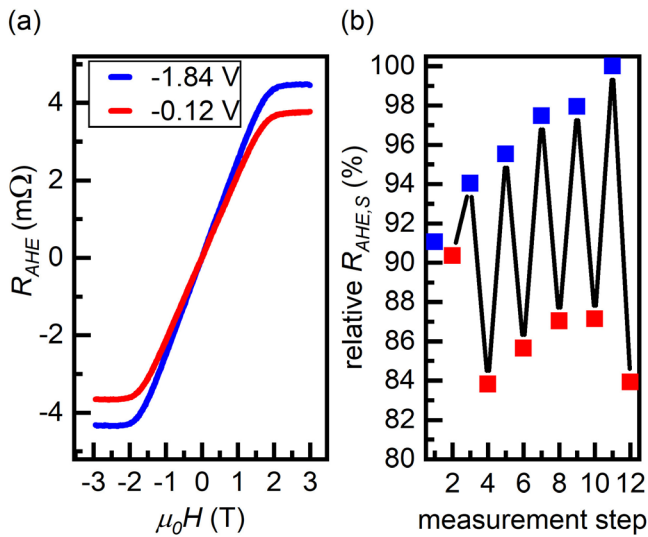


Figure 6. Reversible magneto-ionic change of magnetization in Fe films beyond the ultrathin limit. (a) *In situ* AHE curves as measure for the magnetization curves of electrolytic Fe films produced by FeOOH reduction (figure 3(d), thickness ca. 28 nm) when polarized at -1.84 V (reduction) and -0.12 V (oxidation) in 1 M LiOH. The curves of the 6th reduction and oxidation step are presented. (b) Relative $R_{AHE,S}$ as measure for M_S for 6 repeated reduction and oxidation steps with the measured maximum $R_{AHE,S}$ as reference value. Lines are added as a guide to the eye.

towards larger relative $R_{AHE,S}$ values with increasing measurement steps has been observed in similar systems before and may be related to a stepwise change of the nature of the passive layer during the repeated electro-oxidation steps [9]. The drop of $R_{AHE,S}$ at the last oxidation step may also be connected to a change of the passive layer properties, e.g. a training effect as reported for iron nanoislands in alkaline solution [5]. However, in order to ensure that these effects are systematic also in the

present system, and to understand them in detail, further statistics and *in situ* structural characterization will be required.

The stability of iron oxide/iron in alkaline solution, irrespective of the morphology, is as expected from the E -pH diagram for the present potentials and pH [35, 40]. A similar stability has been experimentally found in previous studies on smooth iron films [9], iron nanoislands [5], and iron nanoparticles [41]. For the latter, the stability has been confirmed for at least several hundred oxidation/reduction cycles [41]. In comparison to magneto-ionic changes in porous Co-Pt microdiscs, the observed magnetization changes in the present study are smaller [25]. However, this is compensated by a better reversibility and a higher overall saturation magnetization of Fe in comparison to Co-Pt.

While voltage-induced full magnetic ON switching starting from FeOOH is readily achieved in the present study, only partial OFF switching of magnetization is observed after re-oxidation. The reason is that during the re-oxidation of the iron films, only a surface layer of few nanometers is affected [9]. A full magnetic OFF switching would become possible when the whole ferromagnetic iron film is transformed back into FeOOH. Indeed, from an electrochemical point of view, the re-oxidation of metal Fe to FeOOH should proceed when applying a suitable oxidation potential (see reactions (1) and (2)). However, the collapse of the porous morphology and formation of a compact iron film impedes the possibility of full re-oxidation, because the electrolyte cannot access all of the buried iron metal. For a fully reversible ON/OFF switching of magnetism in the present case, the porous morphology must be retained. This could be possible by combining FeOOH nanostructures with a 3D carrier structure. An embedding of β -FeOOH in porous carbon, as proposed for battery materials [27], might be a promising avenue. Indeed, in similar FeOOH/carbon nanocomposites, a fully reversible reduction to Fe and re-oxidation to FeOOH nanostructures is already demonstrated [34]. For the implementation of the solid/liquid architectures, in analogy to battery systems, encapsulated architectures containing FeOOH and electrolyte could be designed which can then be magnetically activated by voltage application.

4. Conclusion

We demonstrated the voltage-controlled ON switching of ferromagnetic iron layers starting from paramagnetic FeOOH nanoplatelets via a redox transformation triggered by liquid electrolyte gating. The transformation proceeds via voltage-induced dissolution/redeposition, with the electrodeposited FeOOH structure as iron ion reservoir. The time-dependency of the reduction reaction enables the non-volatile setting of magnetic layers with different total magnetic moments. In the resulting iron layers, with thickness beyond the ultrathin limit, large reversible magneto-ionic changes of magnetization (up to 15%) are achieved. The approach is promising for novel cost-effective routes towards energy-efficient magnetic actuation and magnetoelectronic devices.

Acknowledgments

We acknowledge funding by the DFG (project LE 2558 2-1). We thank S W Boettcher and M Burke (Department of Chemistry and Biochemistry, University of Oregon, USA) and A Eychmueller (Physical Chemistry, Faculty of Chemistry and Food Chemistry, TU Dresden, Germany) for the discussion on the electrodeposition of porous FeOOH and its possible use as magneto-ionic material.

ORCID iDs

Daniel Wolf  <https://orcid.org/0000-0001-5000-8578>
 Kornelius Nielsch  <https://orcid.org/0000-0003-2271-7726>
 Karin Leistner  <https://orcid.org/0000-0002-8049-4877>

References

- [1] Song C, Cui B, Li F, Zhou X and Pan F 2017 Recent progress in voltage control of magnetism: materials, mechanisms, and performance *Prog. Mater. Sci.* **87** 33–82
- [2] Leistner K, Wunderwald J, Lange N, Oswald S, Richter M, Zhang H, Schultz L and Fähler S 2013 Electric-field control of magnetism by reversible surface reduction and oxidation reactions *Phys. Rev. B* **87** 224411
- [3] Bauer U, Emori S and Beach G S D 2013 Voltage-controlled domain wall traps in ferromagnetic nanowires *Nat. Nanotechnol.* **8** 411–6
- [4] Navarro-Senent C, Quintana A, Menéndez E, Pellicer E and Sort J 2019 Electrolyte-gated magnetoelectric actuation: phenomenology, materials, mechanisms, and prospective applications *APL Mater.* **7** 030701
- [5] Duschek K, Petr A, Zehner J, Nielsch K and Leistner K 2018 All-electrochemical voltage-control of magnetization in metal oxide/metal nanoislands *J. Mater. Chem. C* **6** 8411–7
- [6] Quintana A, Menéndez E, Isarain-Chávez E, Fornell J, Solsona P, Fauth F, Baró M D, Nogués J, Pellicer E and Sort J 2018 Tunable magnetism in nanoporous CuNi alloys by reversible voltage-driven element-selective redox processes *Small* **14** 1704396
- [7] Gilbert D A, Grutter A J, Arenholz E, Liu K, Kirby B J, Borchers J A and Maranville B B 2016 Structural and magnetic depth profiles of magneto-ionic heterostructures beyond the interface limit *Nat. Commun.* **7** 11050
- [8] Yan Y N, Zhou X J, Li F, Cui B, Wang Y Y, Wang G Y, Pan F and Song C 2015 Electrical control of Co/Ni magnetism adjacent to gate oxides with low oxygen ion mobility *Appl. Phys. Lett.* **107** 122407
- [9] Duschek K, Pohl D, Fähler S, Nielsch K and Leistner K 2016 Research update: magnetoionic control of magnetization and anisotropy in layered oxide/metal heterostructures *APL Mater.* **4** 032301
- [10] van den Brink A, van der Heijden M A J, Swagten H J M and Koopmans B 2015 Large time-dependent coercivity and resistivity modification under sustained voltage application in a Pt/Co/AlO_x/Pt junction *J. Appl. Phys.* **117** 17C717
- [11] Reichel L, Oswald S, Fähler S, Schultz L and Leistner K 2013 Electrochemically driven variation of magnetic properties in ultrathin CoPt films *J. Appl. Phys.* **113** 143904
- [12] Zehner J, Huhnstock R, Oswald S, Wolff U, Soldatov I, Ehresmann A, Nielsch K, Holzinger D and Leistner K 2019 Nonvolatile electric control of exchange bias by a redox transformation of the ferromagnetic layer *Adv. Electron. Mater.* **5** 1900296
- [13] Bauer U, Yao L, Tan A J, Agrawal P, Emori S, Tuller H L, van Dijken S and Beach G S D 2015 Magneto-ionic control of interfacial magnetism *Nat. Mater.* **14** 174–81
- [14] Bi C, Liu Y, Newhouse-Illige T, Xu M, Rosales M, Freeland J W, Mryasov O, Zhang S, te Velthuis S G E and Wang W G 2014 Reversible control of co magnetism by voltage-induced oxidation *Phys. Rev. Lett.* **113** 267202
- [15] Lee J and Lu W D 2018 On-demand reconfiguration of nanomaterials: when electronics meets ionics *Adv. Mater.* **30** 1702770
- [16] Molinari A, Hahn H and Kruk R 2019 Voltage-control of magnetism in all-solid-state and solid/liquid magnetoelectric composites *Adv. Mater.* **31** 1806662
- [17] Tournier N, Engelhardt A P, Maroun F and Allongue P 2012 Influence of the surface chemistry on the electric-field control of the magnetization of ultrathin films *Phys. Rev. B* **86** 104434
- [18] Zhao S et al 2017 Quantitative determination on ionic-liquid-gating control of interfacial magnetism *Adv. Mater.* **29** 1606478
- [19] Brovko O O, Ruiz-Díaz P, Dasa T R and Stepanyuk V S 2014 Controlling magnetism on metal surfaces with non-magnetic means: electric fields and surface charging *J. Phys.: Condens. Matter* **26** 093001
- [20] Taniguchi K, Narushima K, Yamagishi K, Shito N, Kosaka W and Miyasaka H 2017 Magneto-ionic phase control in a quasi-layered donor/acceptor metal–organic framework by means of a Li-ion battery system *Japan. J. Appl. Phys.* **56** 060307
- [21] Dasgupta S, Das B, Knapp M, Brand Richard A, Ehrenberg H, Kruk R and Hahn H 2014 Intercalation-driven reversible control of magnetism in bulk ferromagnets *Adv. Mater.* **26** 4639–44
- [22] Topolovec S, Jerabek P, Szabó D V, Krenn H and Würschum R 2013 SQUID magnetometry combined with *in situ* cyclic voltammetry: a case study of tunable magnetism of γ -Fe₂O₃ nanoparticles *J. Magn. Magn. Mater.* **329** 43–8
- [23] Dubraja L A, Reitz C, Velasco L, Witte R, Kruk R, Hahn H and Brezesinski T 2018 Electrochemical tuning of magnetism in ordered mesoporous transition-metal ferrite films for micromagnetic actuation *ACS Appl. Nano Mater.* **1** 65–72
- [24] Zhang Q, Luo X, Wang L, Zhang L, Khalid B, Gong J and Wu H 2016 Lithium-ion battery cycling for magnetism control *Nano Lett.* **16** 583–7
- [25] Navarro-Senent C et al 2018 Large magnetoelectric effects in electrodeposited nanoporous microdisks driven by effective surface charging and magneto-ionics *ACS Appl. Mater. Interfaces* **10** 44897–905
- [26] Zou S, Burke M S, Kast M G, Fan J, Danilovic N and Boettcher S W 2015 Fe (oxy)hydroxide oxygen evolution reaction electrocatalysis: intrinsic activity and the roles of electrical conductivity, substrate, and dissolution *Chem. Mater.* **27** 8011–20
- [27] Imtiaz M, Chen Z, Zhu C, Pan H, Zada I, Li Y, Bokhari S W, Luan R, Nigar S and Zhu S 2018 *In situ* growth of β -FeOOH on hierarchically porous carbon as anodes for high-performance lithium-ion batteries *Electrochim. Acta* **283** 401–9
- [28] Benoit C, Bourbon C, Berthet P and Franger S 2006 Chemistry and electrochemistry of nanostructured iron oxyhydroxides as lithium intercalation compounds for energy storage *J. Phys. Chem. Solids* **67** 1265–9

- [29] Nagaosa N, Sinova J, Onoda S, MacDonald A H and Ong N P 2010 Anomalous Hall effect *Rev. Mod. Phys.* **82** 1539–92
- [30] Leistner K, Lange N, Hänisch J, Oswald S, Scheiba F, Fähler S, Schlörb H and Schultz L 2012 Electrode processes and *in situ* magnetic measurements of FePt films in a LiPF₆ based electrolyte *Electrochim. Acta* **81** 330–7
- [31] Cornell R M and Schwertmann U 1996 *The Iron Oxides: Structure, Properties, Reactions, Occurrence, and Uses* (Weinheim: VCH)
- [32] Schrebler Guzmán R S, Vilche J R and Arvía A J 1979 The potentiodynamic behaviour of iron in alkaline solutions *Electrochim. Acta* **24** 395–403
- [33] Casellato U, Comisso N and Mengoli G 2006 Effect of Li ions on reduction of Fe oxides in aqueous alkaline medium *Electrochim. Acta* **51** 5669–81
- [34] Jiang W, Liang F, Wang J, Su L, Wu Y and Wang L 2014 Enhanced electrochemical performances of FeO_x-graphene nanocomposites as anode materials for alkaline nickel-iron batteries *RSC Adv.* **4** 15394–9
- [35] Duschek K, Uhlemann M, Schlörb H, Nielsch K and Leistner K 2016 Electrochemical and *in situ* magnetic study of iron/iron oxide films oxidized and reduced in KOH solution for magneto-ionic switching *Electrochim. Commun.* **72** 153–6
- [36] Allanore A, Lavelaine H, Valentin G, Birat J P and Lapique F 2008 Iron metal production by bulk electrolysis of iron ore particles in aqueous media *J. Electrochem. Soc.* **155** E125
- [37] He Z, Gudavarthy R V, Koza J A and Switzer J A 2011 Room-temperature electrochemical reduction of epitaxial magnetite films to epitaxial iron films *J. Am. Chem. Soc.* **133** 12358–61
- [38] Li D Y and Szpunar J A 1997 A Monte Carlo simulation approach to the texture formation during electrodeposition—II. Simulation and experiment *Electrochim. Acta* **42** 47–60
- [39] Aeppli M, Voegelin A, Gorski C A, Hofstetter T B and Sander M 2018 Mediated electrochemical reduction of iron (oxyhydr-)oxides under defined thermodynamic boundary conditions *Environ. Sci. Technol.* **52** 560–70
- [40] Pourbaix M 1974 *Atlas of Electrochemical Equilibria in Aqueous Solutions* (Houston, TX: NACE International)
- [41] Wang H *et al* 2012 An ultrafast nickel-iron battery from strongly coupled inorganic nanoparticle/nanocarbon hybrid materials *Nat. Commun.* **3** 917